ACCSCIENCE PUBLISHING

International Journal of Bioprinting

RESEARCH ARTICLE

Development of a high-precision 3D bioprinter system using a screw-based dispenser for microextrusion

Supplementary file

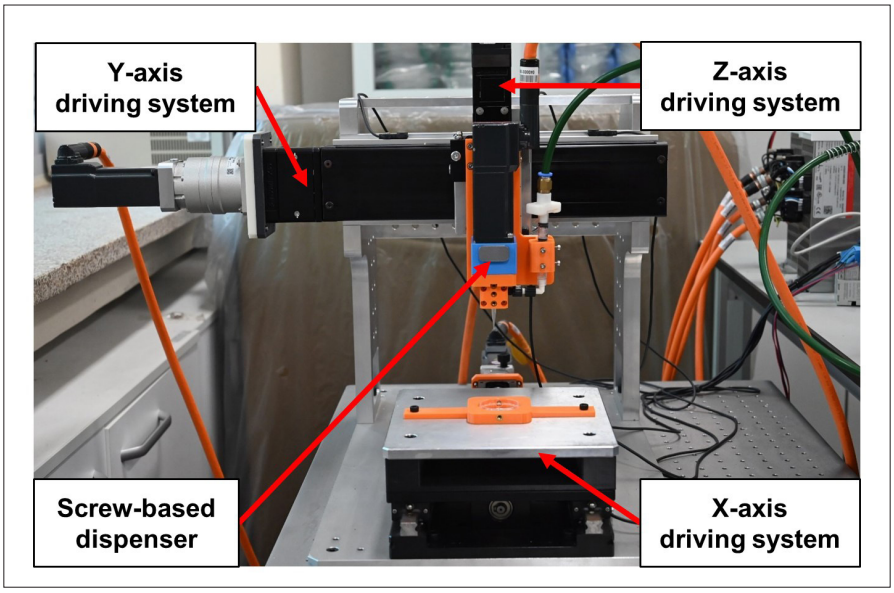

Figure S1. Schematic diagram of the HP-BPS composed of three-axis driving systems and the SB-DP. Abbreviations: HP-BPS, high-precision 3D bioprinter system; SB-DP, screw-based dispenser.

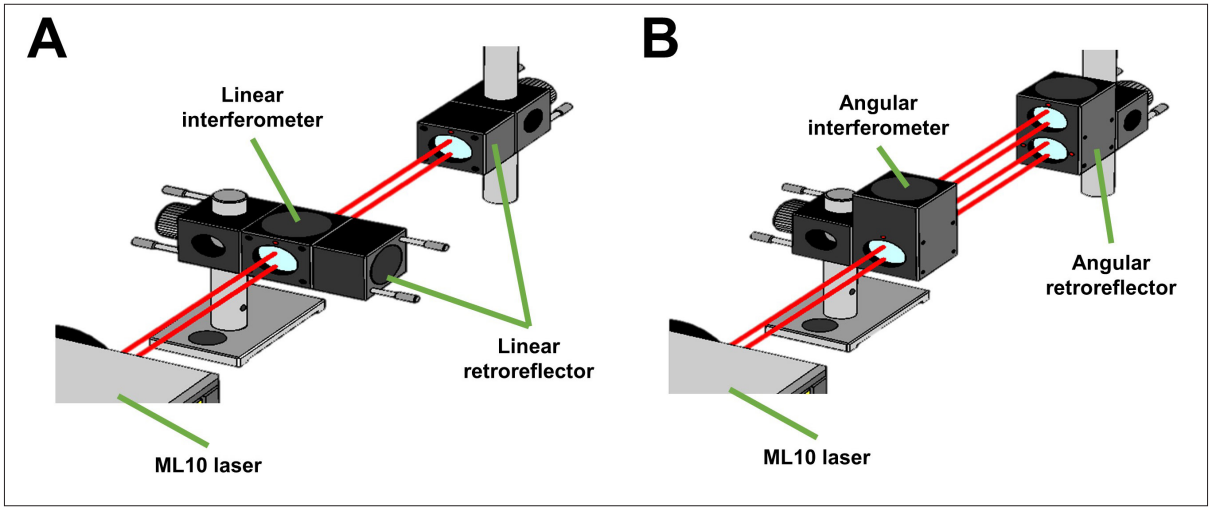

Figure S2. Method for measuring geometric error in the HP-BPS using a laser interferometry system. (A) Method for measuring position error using ML10 laser. (B) Method for measuring angular error using ML10 laser. Abbreviation: HP-BPS, high-precision 3D bioprinter system.

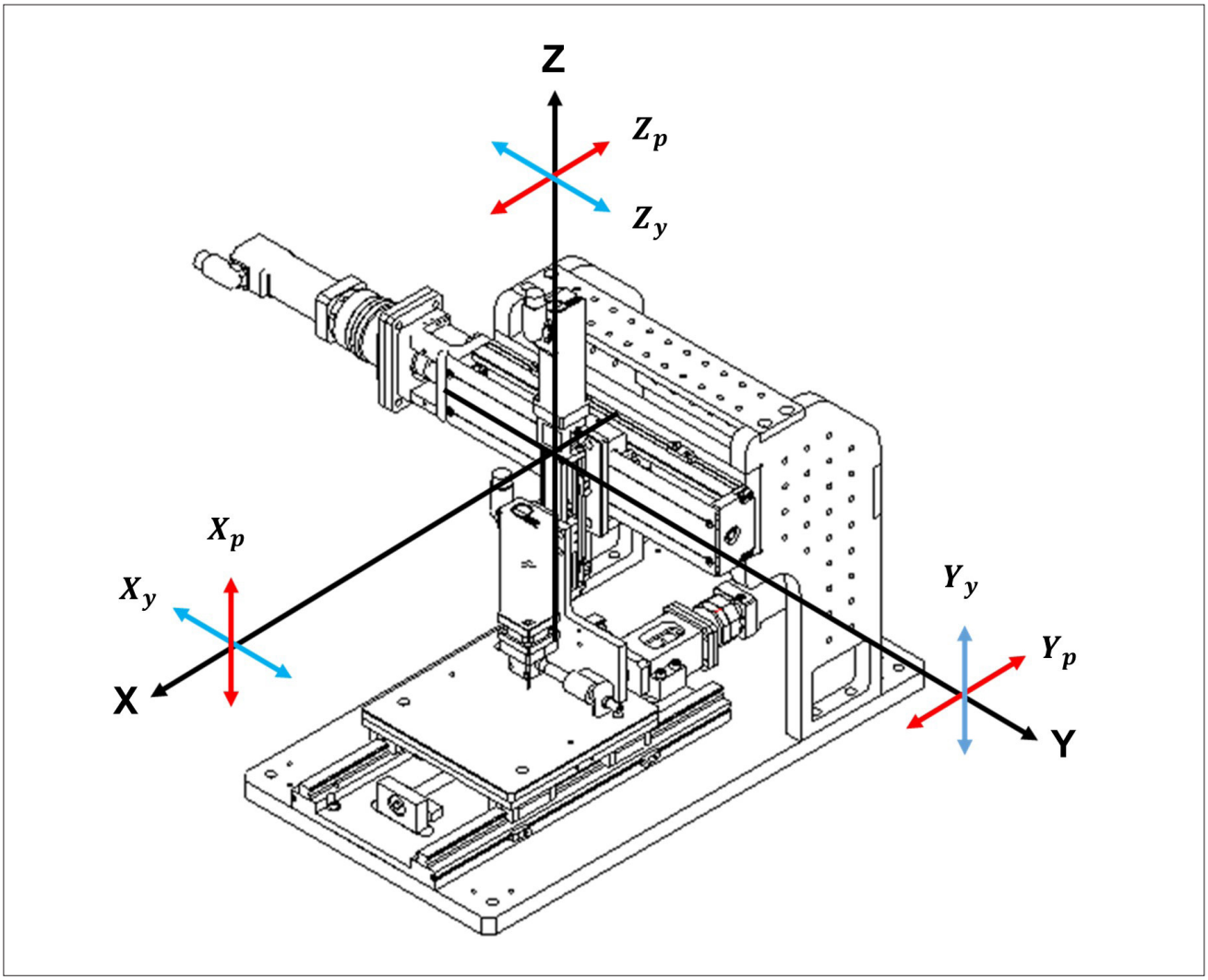

Figure S3. Reference coordinate system of the HP-BPS. The figure illustrated the three-dimensional coordinate system (*X*, *Y*, *Z*) of the HP-BPS, along with the pitch and yaw directions for each axis. The X-axis is presented with its pitch (X_p) and yaw (X_y) components, the Y-axis with its pitch (Y_p) and yaw (Y_y) components, and the *Z*-axis with its pitch (Z_p) and yaw (Z_y) components. Abbreviation: HP-BPS, high-precision 3D bioprinter system.

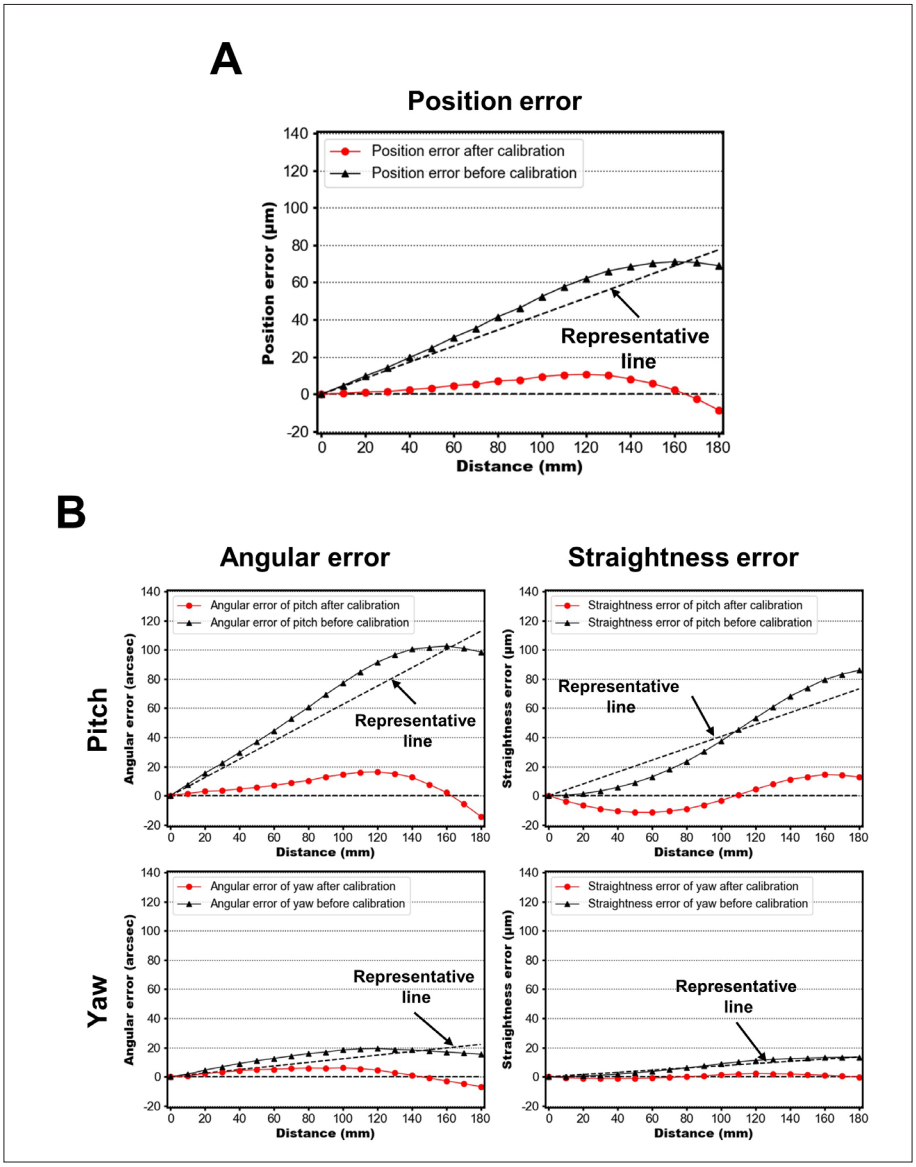

Figure S4. Calibration of geometric errors using the least square method. (A) Calibration of position error. The graph presents position errors before and after calibration along the distance of the axis. The representative line indicates the trend of error before calibration. (B) Calibration of angular and straightness errors in pitch and yaw directions. The upper graphs present the pitch errors, while the lower graphs present the yaw errors. For both pitch and yaw, angular errors (left) and straightness errors (right) are presented before and after calibration. Representative lines indicate the trend of errors before calibration.

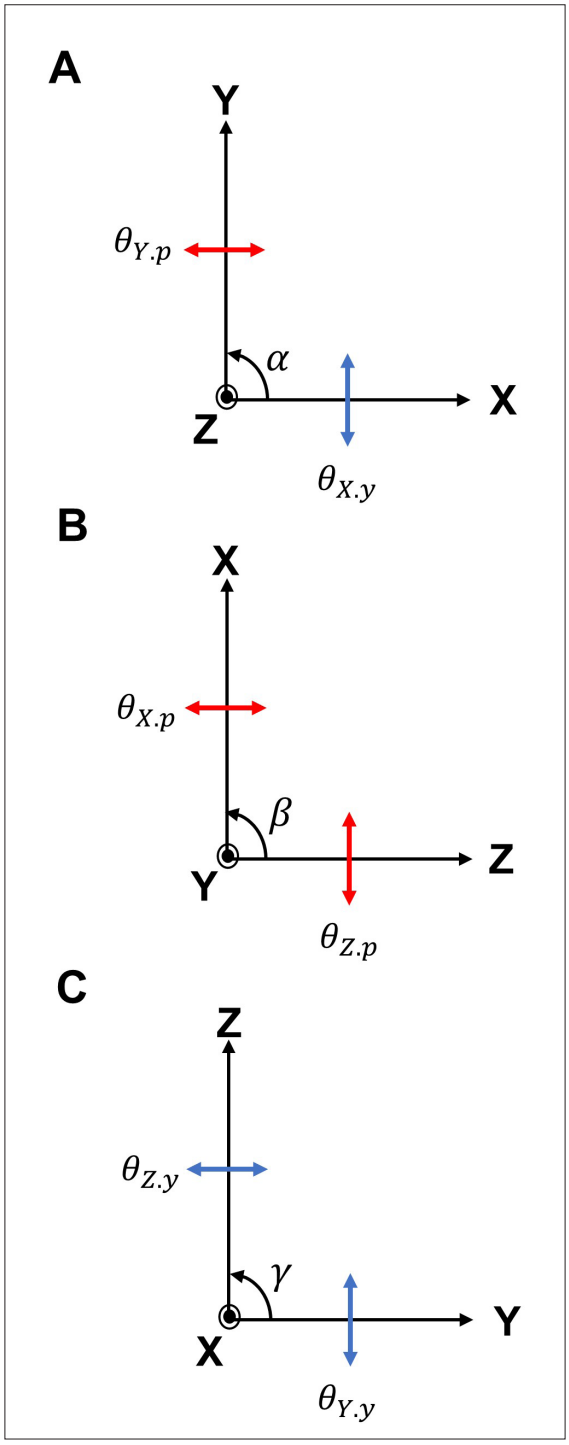

Figure S5. Illustration of minimum squareness error of each plane in the HP-BPS. (A) XY-plane (α), (B) ZX-plane (β), and (C) YZ-plane (γ). These illustrations demonstrate how the angular errors in pitch and yaw directions for each axis contribute to the overall squareness error of the HP-BPS, which is crucial for maintaining precise geometry during the printing process. Abbreviation: HP-BPS, high-precision 3D bioprinter system.

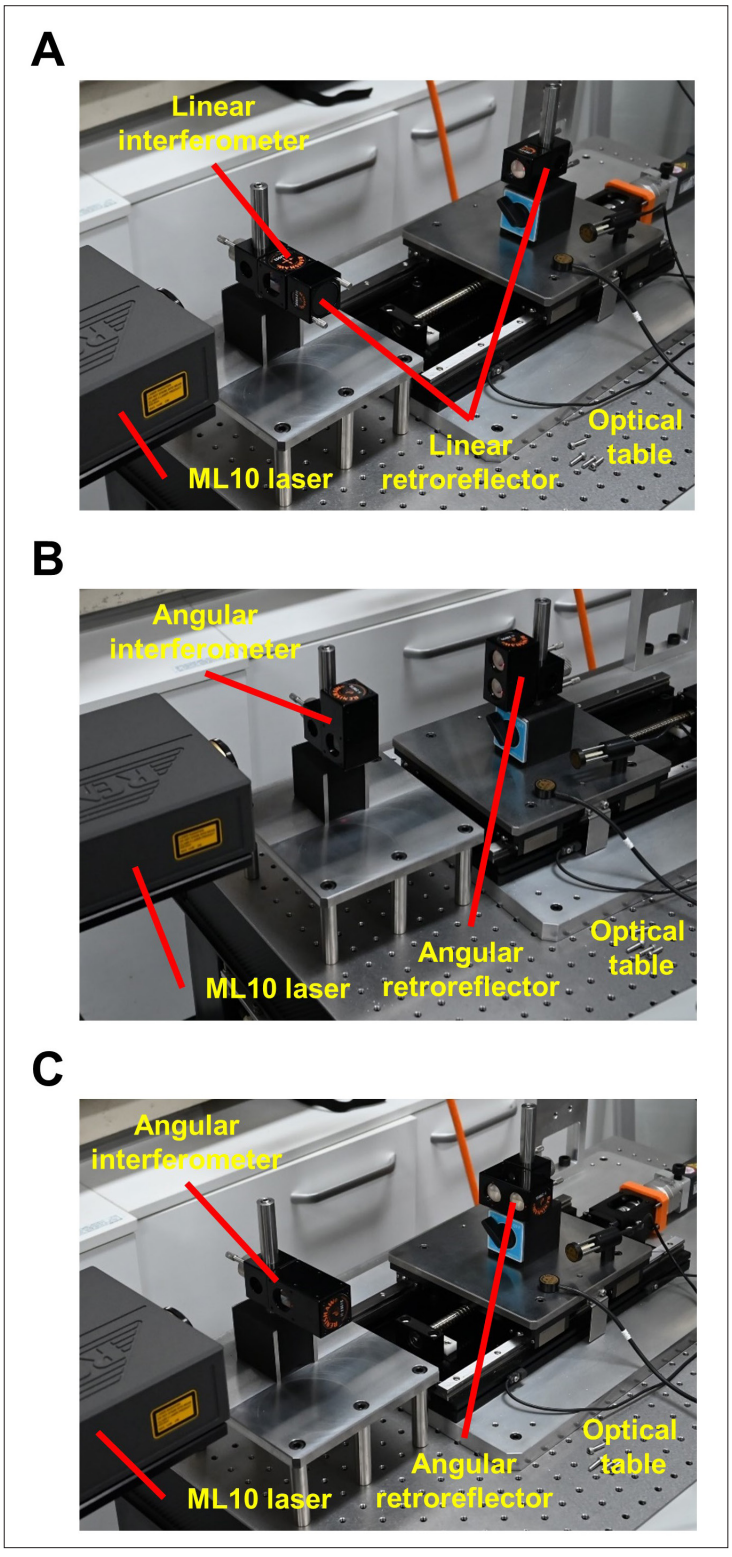

Figure S6. Actual measurements on the *X*-axis driving system using an ML10 laser interferometry system. (A) Position error measurement, (B) angular error measurement of the pitch direction, and (C) angular error measurement of the yaw direction on the *X*-axis driving system. All measurements were conducted on an optical table to minimize external vibrations and ensure accuracy.

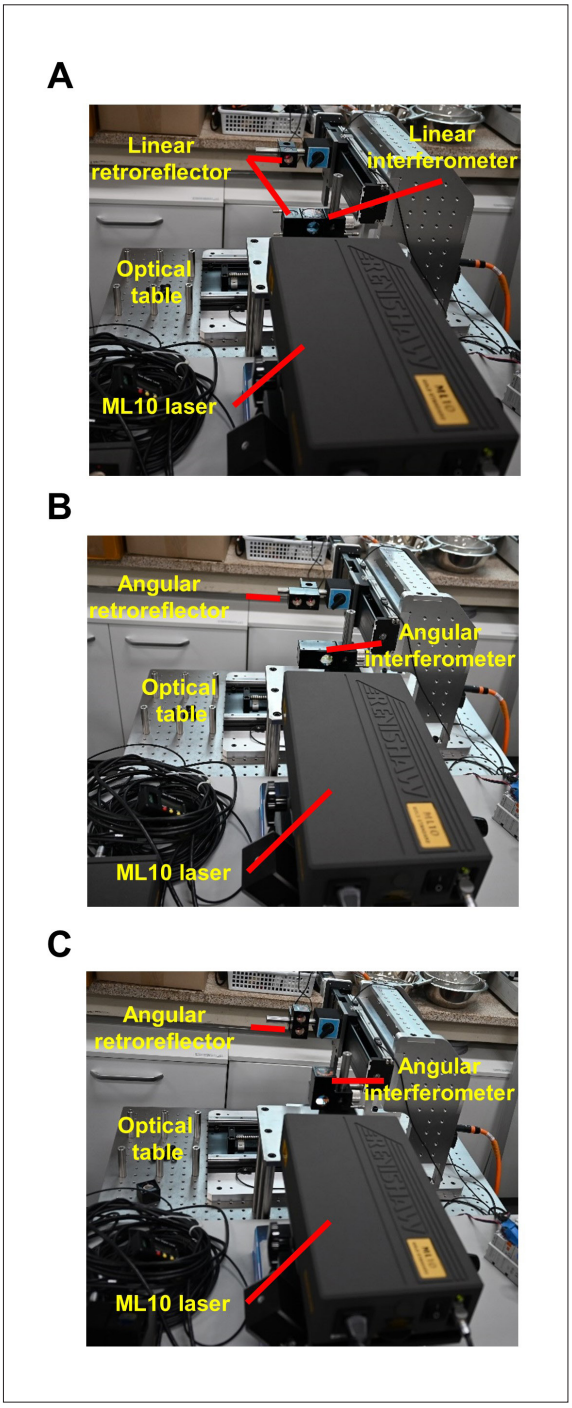

Figure S7. Actual measurements on the *Y*-axis driving system using an ML10 laser interferometry system. (A) Position error measurement, (B) angular error measurement of the pitch direction, and (C) angular error measurement of the yaw direction on the *Y*-axis driving system. All measurements were conducted on an optical table to minimize external vibrations and ensure accuracy.

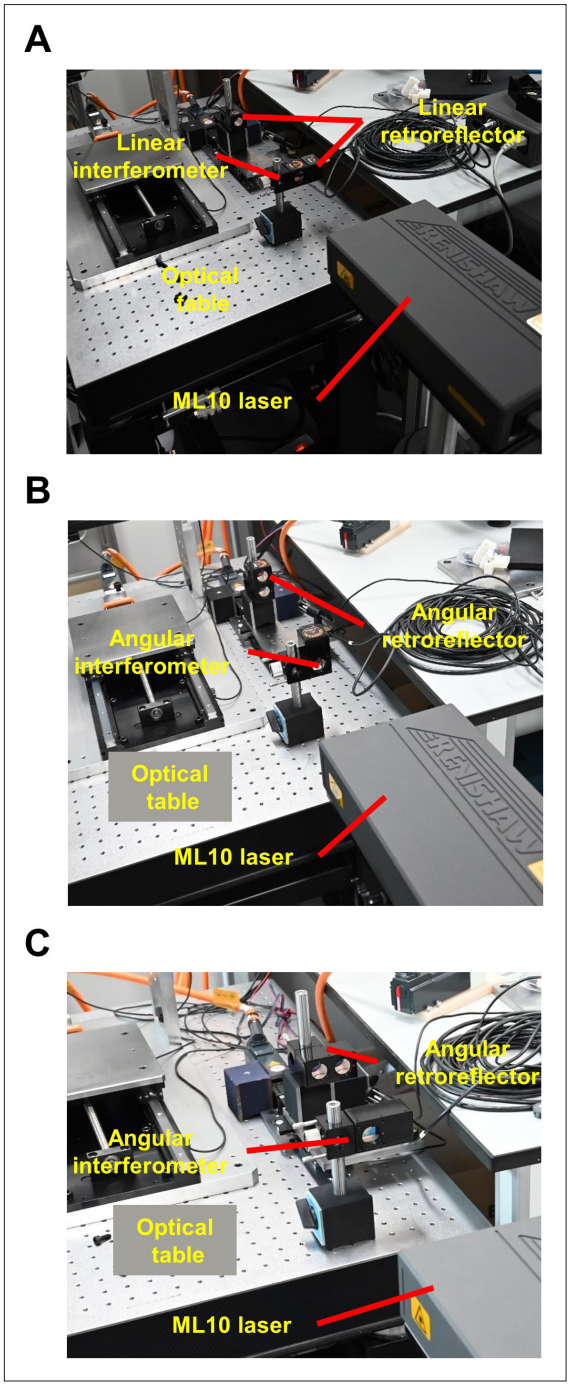

Figure S8. Actual measurements on the *Z*-axis driving system using an ML10 laser interferometry system. (A) Position error measurement, (B) angular error measurement of the pitch direction, and (C) angular error measurement of the yaw direction on the *Z*-axis driving system. All measurements were conducted on an optical table to minimize external vibrations and ensure accuracy.

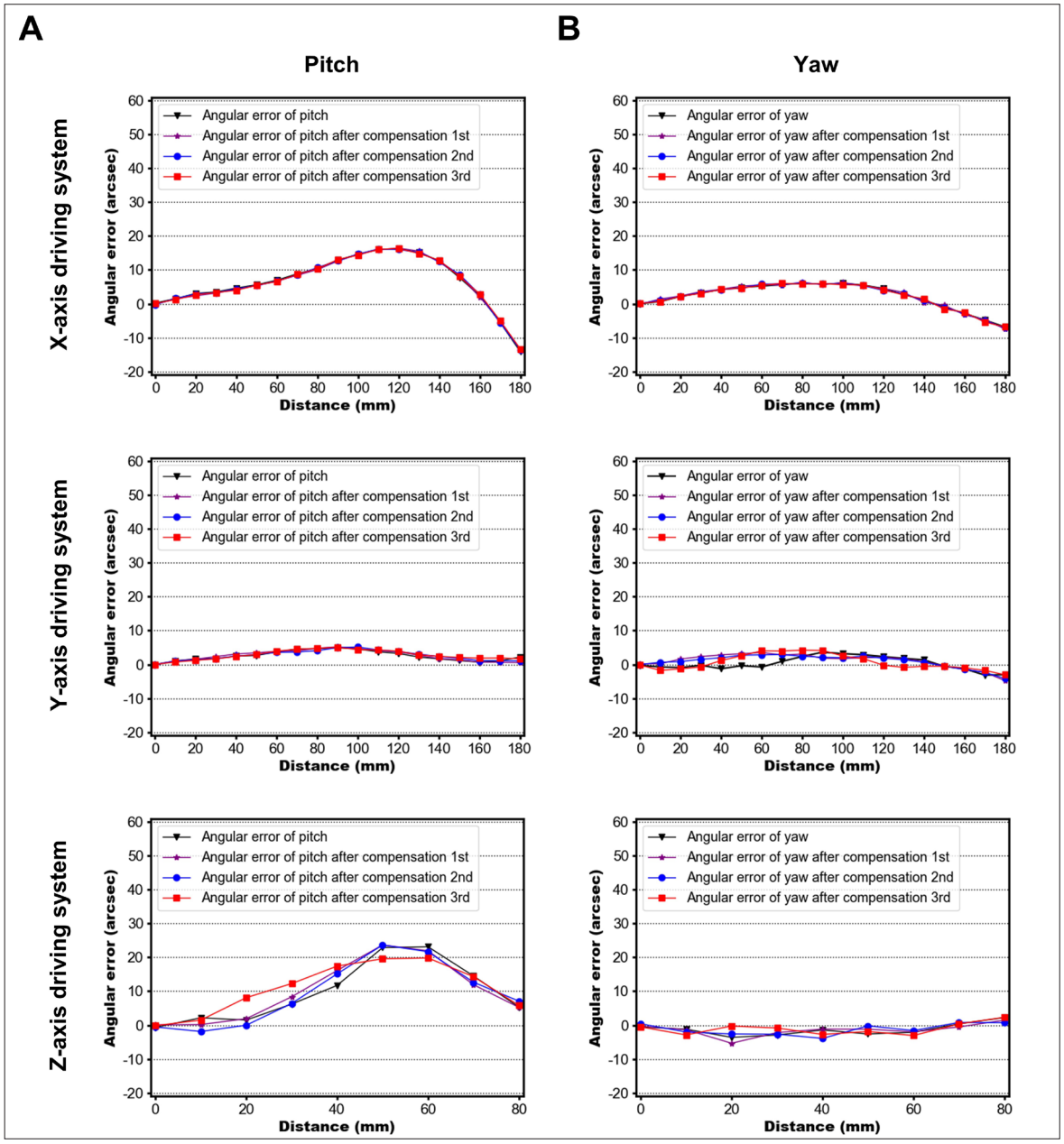

Figure S9. Results of angular error measurements in the HP-BPS through three compensation iterations. (A) Angular error of the pitch direction and (B) angular error of the yaw direction for the *X*-, *Y*-, and *Z*-axis driving systems. This data demonstrate the effectiveness of the compensation iterations in minimizing angular errors, which is crucial for maintaining high precision in the 3D bioprinting process across all axes of motion. Abbreviation: HP-BPS, high-precision 3D bioprinter system.

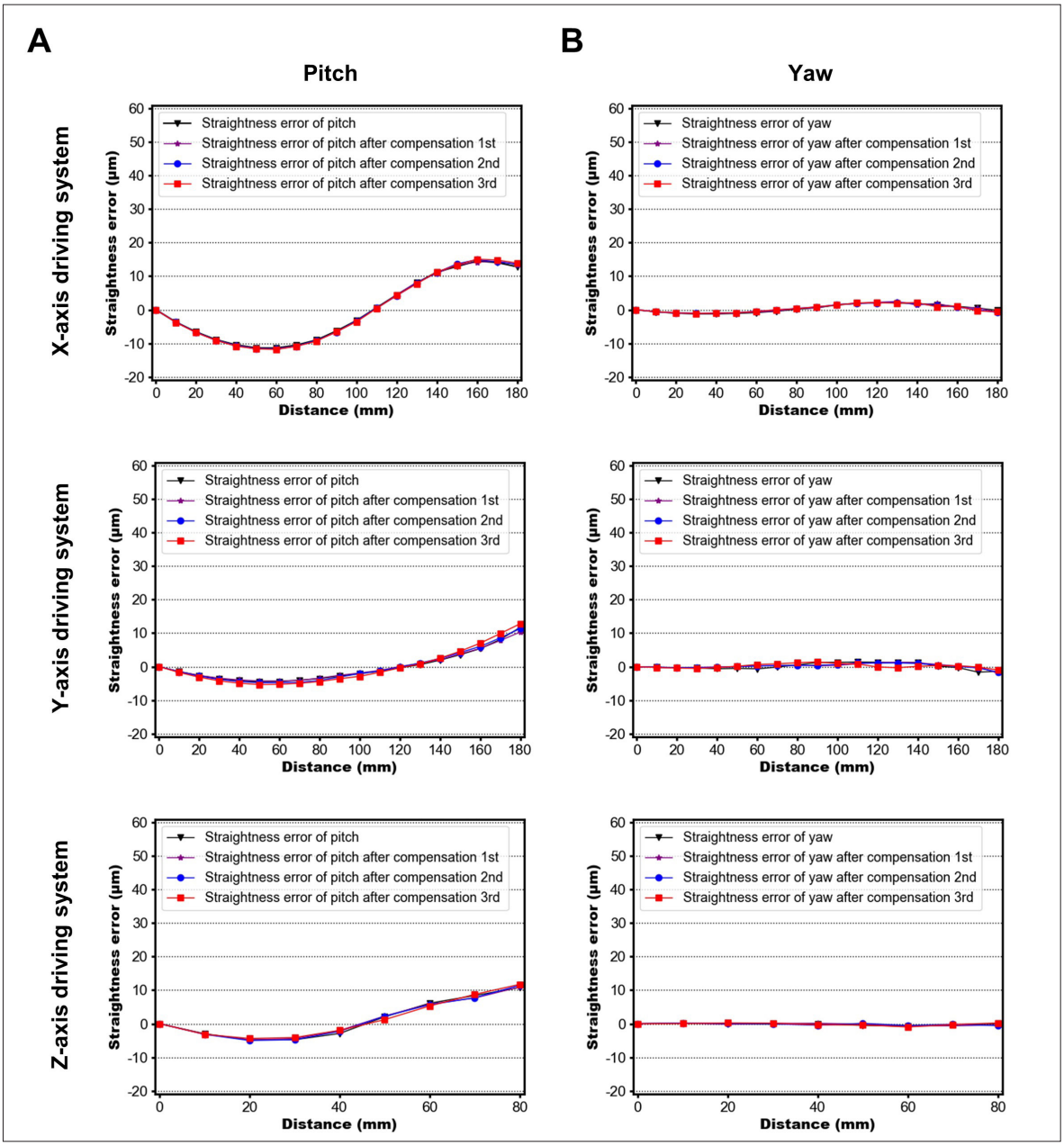

Figure S10. Results of straightness error measurements in the HP-BPS through three compensation iterations. (A) Straightness error of the pitch direction and (B) straightness error of the yaw direction for the *X*-, *Y*-, and *Z*-axis driving systems. This data demonstrate the effectiveness of the compensation iterations in reducing straightness errors, which is crucial for maintaining high precision and accuracy in the 3D bioprinting process across all axes of motion. Abbreviation: HP-BPS, high-precision 3D bioprinter system.

Table S1. Repeatability of the *X*-, *Y*-, and *Z*-axis driving systems in the HP-BPS

Repeatability of parts on the axis driving system	*X*-axis	*Y*-axis	*Z*-axis
Repeatability of linear actuator (μm)	±3	±3	±3
Repeatability of servo motor (μm)	±0.02	±0.04	±0.02
Repeatability of coupling (μm)	±0	±0	±0
Repeatability of reducer (μm)	±0.69	±1.39	-
Repeatability of axis driving system (μm)	±3.71	±4.43	±3.02

Note: The table presents the repeatability measurements for various components (linear actuator, servo motor, coupling, and reducer) and the overall axis driving system for each axis. The overall repeatability of each axis driving system is presented in the last row. Abbreviation: HP-BPS, high-precision 3D bioprinter system.

Table S2. Environmental conditions during geometric error measurements of each axis driving system of the HP-BPS using laser interferometry system

Axes of measurement	Driving system		
	X-axis	*Y*-axis	*Z*-axis
Temperature (°C)	21.56 ± 0.32	18.12 ± 0.35	19.62 ± 0.39
Pressure (mbar)	1015.63 ± 0.78	1021.06 ± 0.99	1017.61 ± 0.86
Relative humidity (%)	27.04 ± 1.21	32.12 ± 2.75	20.50 ± 3.01
Vibration criterion		Class B	

Note: The table presents the temperature, pressure, and relative humidity data for the *X*-, *Y*-, and *Z*-axis driving systems during laser interferometry system measurements. Data are presented as mean ± standard deviation. Conditions were relatively consistent across axes. The vibration criterion was Class B for all measurements, ensuring stable measurement conditions. Abbreviation: HP-BPS, high-precision 3D bioprinter system.

Table S3. Motion error with and without an installed reducer

Motion error	Circular diameter (mm)		
	5	0.5	0.1
Reducer installed (μm)	±9.98	±10.86	±12.43
Reducer not installed (μm)	±214.22	±339.97	±197.84

Note: The table compared the motion errors for three different circular diameters (5, 0.5, and 0.1 mm) under two conditions: with a mounted reducer and without an installed reducer. The results demonstrated significantly lower motion errors when the reducer was installed, highlighting its importance in improving precision across various movement scales in the HP-BPS. Abbreviation: HP-BPS, high-precision 3D bioprinter system.

Table S4. Geometric error measurements on the *X*-, *Y*-, and *Z*-axis driving systems before applying compensation

Error type	Driving system		
	X-axis	*Y*-axis	*Z*-axis
Position error (μm)	±10.6 (±0.35)	±3.6 (±0.25)	±12.4 (±0.46)
Straight error of pitch (μm)	±14.5 (±0.10)	±11.7 (±0.04)	±10.8 (±0.17)
Straight error of yaw (μm)	±2.2 (±0.09)	±1.6 (±0.08)	±0.7 (±0.09)
Angular error of pitch (arcsec, ″)	±16.3 (±0.30)	±4.9 (±0.15)	±23.1 (±1.46)
Angular error of yaw (arcsec, ″)	±6.8 (±0.26)	±3.6 (±0.20)	±3.6 (±1.12)

Note: The table presents five types of errors for each axis: position error, straightness errors (pitch and yaw), and angular errors (pitch and yaw). Data are presented as ±error (±standard deviation).

Table S5. Geometric error measurements on the *X*-, *Y*-, and *Z*-axis driving systems after the first compensation

Error type	Driving system		
	X-axis	*Y*-axis	*Z*-axis
Position error (μm)	±0.9 (±0.18)	±0.9 (±0.16)	±2.3 (±0.42)
Straight error of pitch (μm)	±14.5 (±0.12)	±10.3 (±0.16)	±11.0 (±0.36)
Straight error of yaw (μm)	±2.4 (±0.04)	±1.9 (±0.13)	±0.7 (±0.13)
Angular error of pitch (arcsec,″)	±16.4 (±0.29)	±5.2 (±0.48)	±23.7 (±2.29)
Angular error of yaw (arcsec,″)	±7.5 (±0.18)	±4.8 (±0.38)	±5.4 (±0.90)

Note: The table presents updated values for five types of errors across each axis: position error, straightness errors (pitch and yaw), and angular errors (pitch and yaw). Data are presented as ±error (±standard deviation).

Table S6. Geometric error measurements on the *X*-, *Y*-, and *Z*-axis driving systems after the second compensation

Error type	Driving system		
	X-axis	*Y*-axis	*Z*-axis
Position error (μm)	±0.8 (±0.11)	±0.7 (±0.18)	±1.95 (±0.31)
Straight error of pitch (μm)	±14.9 (±0.28)	±11.4 (±0.14)	±11.5 (±0.12)
Straight error of yaw (μm)	±2.2 (±0.10)	±1.7 (±0.12)	±0.6 (±0.19)
Angular error of pitch (arcsec,″)	±16.2 (±0.64)	±5.1 (±0.29)	±23.7 (±1.61)
Angular error of yaw (arcsec,″)	±7.1 (±0.26)	±4.2 (±0.29)	±3.9 (±1.22)

Note: The table presents updated values for five types of errors across each axis: position error, straightness errors (pitch and yaw), and angular errors (pitch and yaw). Data are presented as ±error (±standard deviation).

Table S7. Minimum squareness error for each plane in the HP-BPS

Plane	Minimum squareness error (arcsec,″)
XY (α)	±11.8
ZX (β)	±36.1
YZ (γ)	±7.3

Note: The table presents the minimum squareness errors for three orthogonal planes. The values represent the smallest possible deviations from perfect perpendicularity between axes in each plane, measured in arcseconds. These measurements are crucial for understanding and optimizing the overall geometric accuracy of the HP-BPS. Abbreviation: HP-BPS, high-precision 3D bioprinter system.

Table S8. Input and output parameters in the printing condition process

No	Input		Output
	Screw rotation rate (rev/mm)	Printing speed (mm/min)	Strut diameter (μm)
1	0.025	100	244.68
2	0.025	100	223.40
3	0.025	100	260.64
4	0.025	100	281.82
5	0.025	100	218.58
6	0.025	300	220.57
7	0.025	300	241.49
8	0.025	300	249.13
9	0.025	500	234.04
10	0.025	500	255.32
11	0.1	100	521.28
12	0.1	100	585.11
13	0.1	100	553.19
14	0.1	100	542.55
15	0.1	100	553.90
16	0.1	300	404.26
17	0.1	300	446.94
18	0.1	300	489.47
19	0.1	300	436.17
20	0.1	300	446.81
21	0.1	500	457.45
22	0.1	500	361.70
23	0.1	500	425.53
24	0.1	500	457.45
25	0.1	500	404.26
26	0.2	100	648.94
27	0.2	100	595.74
28	0.2	100	691.49
29	0.2	100	638.30
30	0.2	100	648.94
31	0.2	300	574.47
32	0.2	300	585.11
33	0.2	300	553.07
34	0.2	300	553.19
35	0.2	300	563.83
36	0.2	500	521.28
37	0.2	500	531.27
38	0.2	500	500.61
39	0.2	500	478.72
40	0.2	500	531.91

Table S9. ANOVA table of strut diameter

Source	Sum of squares	Degrees of freedom	Mean square	*F*	*p*
Model	750,109.33	5.0	150,021.87	152.79	<0.0001
A	214,457.60	1.0	214,457.60	218.41	<0.0001
B	4812.25	1.0	4812.25	4.90	0.0337
AB	12,589.10	1.0	12,589.10	12.82	0.0011
A^2	72,149.10	1.0	72,149.10	73.48	<0.0001
B^2	3,718.35	1.0	3718.35	3.79	0.0600
Residual	33,384.44	34.0	981.90	-	-
Lack of fit	10,107.51	3.0	3369.17	4.49	0.0100
Pure error	23,276.93	31.0	750.87	-	-
Cor total	783,493.77	39.0	-	-	-

Note: A refers to the screw rotation rate; B refers to the print speed. The R^2 value is 95.74%; the adjusted R^2 value is 95.11%. Abbreviation: ANOVA, analysis of variance.